

# Effects of different dust particles on calcium current in the neurons of dorsal root ganglia of rats<sup>☆</sup>

Yong Mei, Haibing Yang, Jingzhi Sun, Xiao Yin, Xiang Guo, Zhenglun Wang, Lei Yang\*

Department of Occupational and Environmental Health, School of Public Health, Tongji Medical College, Huazhong University of Science & Technology, Wuhan, Hubei 430030 China

Received September 9, 2007

---

## Abstract

**Objective.** To investigate the roles of voltage-dependent calcium channel in occupational pulmonary diseases by measurement of calcium current of dorsal root ganglia (DRG) neuron after exposure to different particulates. **Methods.** Particulates were sampled with respirable dust sampler from the coke oven plant and steel plant. After DRGs were exposed to different particulates in different concentrations (0, 5, 15, 45, 135  $\mu\text{g/ml}$ ) for 2 hours, high-voltage-activated (HVA) calcium current was recorded with whole cell patch clamp recording technique. **Results.** After exposure to quartz, the maximum activated calcium current ( $I_{\text{Ca}}$ ) of DRG increased with the increase of quartz concentration. At the quartz concentration of 135  $\mu\text{g/ml}$ ,  $I_{\text{Ca}}$  was as high as  $-95.89 \pm 38.82$  pA/pF and significantly higher than that of the control and other test groups and had a certain relation of dose-response. The maximum rise slope of calcium current in the coke oven plant (5  $\mu\text{g/ml}$ ) and steel plant particle (135  $\mu\text{g/ml}$ ) groups were significantly higher than that of their controls. The values of  $V_{1/2}$  moved to right about 4 to 6 mV caused by the three types of particulates. **Conclusion.** The quartz caused DRG HVA calcium channel current density increased significantly, while the coke oven plant particulates and steel plant particulates induced a significant increase of maximum activation slope of calcium current. A new approach, to study the effects of different particulates on calcium channel of target cells, has been found for further exploration of mechanism about occupational injury such as inflammation, lung fibrosis and even tumor. [Life Science Journal. 2007; 4(4): 10 – 14] (ISSN: 1097 – 8135).

**Keywords:** particulates; dorsal root ganglia; calcium channel; patch clamp; whole cell recording technique

---

## 1 Introduction

Non-choline and non-adrenaline nerves dominate the nerves of respiratory system. These nerves root in brain stem, spinal cord and trachea nerve<sup>[1]</sup>. For example, the nerve fibers of dorsal root ganglion, trigeminal and neck ganglion are distributed in respiratory system, which contact with respiratory cells and expose to respirable pollutants (such as dust). Dust particles affect these target organizations and cells and trigger a series of biological reactions<sup>[2]</sup>. However, few references concern about the role of sensory nerves in inflammation and pulmonary fibrosis caused by dust<sup>[3]</sup>. Some studies showed that

there are many receptors in sensory nerves, and respiratory epithelium, which can be activated by stimulus (such as acid, chemical substance, plant toxins and capsaicin, etc.). Once these receptors are activated, the ion concentration inward and outward cells will change, which may induce nerve inflammation<sup>[4]</sup>. And then early inflammation events will occur. Inflammation, particularly persistent inflammation, is believed to be the common course of lung injury and also a key to induce pulmonary fibrosis<sup>[5]</sup>. The aim of this study was to use whole cell recording patch clamp technique to explore the significance of the changes in calcium current.

## 2 Materials and Methods

### 2.1 Cell separation and cultivation

Glass flake preparing: coating with 0.15 mol/L Poly-L-

---

\*Supported by The National Natural Science Foundation of China (No.30671743).

\*Corresponding author. Email: Leiyang@mails.tjmu.edu.cn

Lysine (Sigma, USA), and exposure to ultraviolet for 30 minutes. Dorsal root ganglion cells came from male and female Sprague-Dawley rats (150 – 250g) that were anesthetized with pentobarbital sodium (50 mg/kg). The cells were isolated aseptically and washed several times in a cold (4 °C) modified Hank's balanced salt solution containing: 130 mmol/L NaCl, 5 mmol/L KCl, 0.3 mmol/L  $\text{KH}_2\text{PO}_4$ , 4.0 mmol/L  $\text{NaHCO}_3$ , 0.3 mmol/L  $\text{Na}_2\text{HPO}_4$ , 5.6 mmol/L D-glucose, and 10 mmol/L HEPES (Sigma). They were then incubated for 35 minutes at 37 °C in Hanks' balanced salt solution containing 0.125% trypsin (Amresco), and 0.3% collagenase Type I (Gibico). The cells were cultured in DMEM (Gibico) supplemented with 10% fetal bovine serum (Gibico). The cells were plated on poly-D-lysine coated glass flake and cultured overnight at 37 °C in a water saturated atmosphere with 5%  $\text{CO}_2$ . Patch-clamp experiments were performed on cells cultured for 12 – 24 hours.

## 2.2 Dust collection, handling and grouping

Three kinds of dust were: 1) Standard quartz dust, provided by the Chinese CDC. The purity was 99% and the aerodynamics diameter (97%) was  $\leq 5 \mu\text{m}$ ; 2) The coke oven plant dust were gathered in the workplace of plant furnace top. The aerodynamics diameter was  $\leq 7.07\mu\text{m}$ ; 3) The steel plant respirable dust was sampled in the workplace by Germany dust samplers (MPG II). The aerodynamics diameter was  $\leq 5 \mu\text{m}$ . After the three kinds of dust were soaked, ultrasonic shocked, filtrated, centrifuged and low-temperature dried, required by cells, fluid configuration into concentration. Divided into three categories according to dust groups, each divided into five concentration groups (0, 5, 15, 45, 135  $\mu\text{g/ml}$ ). DRG exposed to the dust concentration groups.

## 2.3 The external solution and the internal solution

The external solution used for  $\text{Ca}^{2+}$  channel current measurement consisted of: 110 mmol/L Choline-Cl (Sigma), 20 mmol/L TEACl (Sigma), 10 mmol/L  $\text{BaCl}_2$ , 2.0 mmol/L  $\text{MgCl}_2$ , 10 mmol/L HEPES, and 20 mmol/L D-glucose, adjusted to pH 7.4 with CsOH.  $\text{Ba}^{2+}$  was used as the charge carrier. The internal solution consisted of: 64.0 mmol/L CsF, 64.0 mmol/L CsCl (Amresco), 0.1 mmol/L  $\text{CaCl}_2$ , 2.0 mmol/L  $\text{MgCl}_2$ , 10.0 mmol/L EGTA (Amresco), 10.0 mmol/L HEPES and 5.0 mmol/L Tris-ATP, pH adjusted to 7.2 with CsOH.

## 2.4 Electrophysiological recordings

For whole-cell voltage-clamp experiments we used glass pipettes (R-6 borosilicate, Drummond Scientific Company, Broomall, PA) with resistances from 1 to 5

$\text{M}\Omega$ , 0.5 – 1.5  $\mu\text{m}$  in diameter. Whole cell patch-clamp recordings were performed with an Axopatch-200B patch clamp amplifier (Axon Instruments, Foster City, CA) and the output was digitized with a Digidata 1322A converter (Axon Instruments). The sampling rate was 10 kHz (without filtering). For voltage-clamp experiments, the capacitance and the series resistance were compensated 70% – 90% usually. When the voltage-clamp errors were  $\geq 5 \text{ mV}$  after compensation the data were excluded out. All data collection and analysis were carried out with pCLAMP 9.0 software (Axon Instruments).

The  $I_{\text{Ca}}$  was recorded only when the currents became stable, that was, the fluctuation was less than 10%. All experiments were carried out at room temperature (22 – 24 °C).

## 2.5 Data analyses

The peak conductance (G) of  $I_{\text{Ca}}$  at each potential was calculated from the corresponding peak current by using the equation:  $G = I/(E - E_{\text{Rev}})$ , where  $E_{\text{Rev}}$  was the reversal potential of  $I_{\text{Ca}}$ , I was the peak current amplitude of  $I_{\text{Ca}}$ , and E was the membrane potential.

Normalized peak conductance ( $G/G_{\text{max}}$ ) was fitted with the Boltzmann relation:  $G/G_{\text{max}} = 1 + \exp(V_{1/2} - V_m)/k$ , where  $V_{1/2}$  was the membrane potential at which 50% of activation of the current was observed,  $V_m$  was the pre-pulse membrane potential, and k was the slope of the function.

All data were presented as the means  $\pm$  SEM of experiments and error bars were plotted as SEM, and analyzed for statistical significance using the paired Student's *t* test. *P* value of less than 0.05 was considered significant.

## 3 Results

### 3.1 The effect of different dusts on DRG high-voltage-activated (HVA) calcium currents

Table 1 and Figure 1 showed that the HVA DRG activated calcium currents increased with the quartz concentration rising. When quartz dust concentration reached 135  $\mu\text{g/ml}$ , the HVA DRG activated calcium currents was clearly higher than that of the control group and the low-dose group. There was a significant differences ( $P < 0.05$ ) and a dose-response relationship ( $P < 0.01$ ,  $R^2 = 0.99$ ).

### 3.2 Effects of different dusts on the activation slope of DRG HVA calcium currents

Table 2 showed that the activation slope of DRG HVA calcium currents in 5  $\mu\text{g/ml}$  coke plant dust group was higher than that of the others in the same group ( $P < 0.05$ ). The activation slope of DRG HVA calcium currents in

**Table 1.** DRG HVA calcium currents in different dust (pA/pF)

Group	Dust concentration ( $\mu\text{g/ml}$ )				
	0	5	15	45	135
Quartz	$-37.50 \pm 29.66$	$-40.49 \pm 28.97$	$-38.81 \pm 20.60$	$-59.20 \pm 29.10^*$	$-95.89 \pm 38.82^*$
Coke plant dust	$-49.13 \pm 30.87$	$-62.89 \pm 41.35$	$-71.83 \pm 33.51$	$-52.17 \pm 17.04$	$-67.85 \pm 28.67$
Steel plant dust	$-33.61 \pm 27.84$	$-55.06 \pm 16.73$	$-48.51 \pm 17.16$	$-53.61 \pm 25.04$	$-40.01 \pm 21.03$

\*: vs. 0  $\mu\text{g/ml}$ ,  $P < 0.05$ .

135  $\mu\text{g/ml}$  steel plant respirable dust was significant increased than that of 0  $\mu\text{g/ml}$  and other concentrations ( $P < 0.05$ ).

### 3.3 Effects of quartz dust on the DRG HVA calcium currents I-V curve

Figure 2 showed that the calcium currents increased, especially between  $-10$  mV to  $30$  mV in silica groups of  $45$   $\mu\text{g/ml}$  and  $135$   $\mu\text{g/ml}$ , but there was no obvious change about the shape of I-V curve. The activation potential was  $0$  mV.

### 3.4 Effects of quartz on DRG HVA calcium currents with time

In order to record the calcium current,  $-40$  mV holding potential,  $150$  ms interval and  $0$  mV depolarization square pulse were performed. After fast, slow capacitance and series impedance were compensated, and the current was recorded in 1, 2, 3, 5, 7, 10, 15, 20, 25, 30 minutes. The current density was stable within 5 – 20 minutes and weakens after 25 minutes. By comparison with control group, there was no significantly difference about the current density.

### 3.5 Effects of stable state activation curve by quartz dust on DRG HVA calcium currents

HVA calcium currents activate curve fitting results showed that the curve fitting was perfect and the coefficient was  $\geq 0.97$ . Different dusts could cause  $V_{1/2}$  significant increase ( $P > 0.05$ ) and  $V_{1/2}$  drift to the positive direction about  $4 - 6$  mV. The curve slope did not change significantly (Figure 3).

### 3.6 Effects of stable state activation curve by silica dust on DRG HVA calcium currents

Figure 3 showed that the curve fit well and the adjusted determinate coefficient were over  $0.97$ .  $V_{1/2}$  value of HVA calcium current steady-activation-curve in DRG removed from  $4 - 6$  mV to right of X-axis. The difference was significant by comparison with the control, but there was no certain relation with dose ( $P > 0.05$ ) and slope  $k$  didn't change ( $P > 0.05$ ).

## 4 Discussion

Sensory nerves, originating from dorsal root ganglia (DRG), extend their terminals into the nasal and pulmonary epithelium and belong to nociception primary afferent sensory nerve. There are many types of ion channel on the bodies and nerve terminals, which plays important roles in sensory information transfer. The voltage-activated calcium channels, including six subtypes of L, N, T, P, Q and R, are in charge of calcium ion inflow, among which L subtype calcium channel is one of the most important, and is related to modulation of transmittance release and genetic expression. L subtype calcium channel is very sensitive to high voltage.

When the membrane potential is beyond negative  $40$  mV, L-type calcium channel is easy to be activated. L-type calcium channel open and calcium ion inflow quickly. The voltage dependence of N-type calcium channel is slightly less than that of L-type calcium channel and it is easy to be activated under rapid depolarization; but it deactivates quickly, too<sup>[6]</sup>. Both of them are high-voltage-activated and distribute on the surface of neurons membrane.

This study showed that the calcium channel was affected after exposure to dust. DRG HVA inward calcium current increased significantly after exposed to silica. The maximum activation slope of calcium current rose when DRG neurons were exposed to dust of the coke oven plant and steel plant. The change of ionic current by channel reflects the molecular action of ion channel on cellular membrane. So HVA calcium current increase indicated that molecular structure and function of HVA calciphorin were influenced by particulate matter. The protein of calcium channel is composed of subtype units including alpha 1, alpha 2, beta, gamma and delta. There are four homedomains in alpha 1 subtype and there are six transmembrane domains (S1 – S6) in every homedomain. S4 is the area for potential sensitivity and directly regulates calcium channel activity by positive charge of spiral arrangement outside of alpha spiral<sup>[7]</sup>. The positive charge may be neutralized or attracted by the negative charge out of silica particle<sup>[8]</sup>, which makes spiral rotate and sensitivity of S4 to potential increase, and the

**Table 2.** The activation slope of DRG HVA calcium currents in different dust (pA/pF)

Group	Dust concentration (µg/ml)				
	0	5	15	45	135
Quartz	9.22 ± 4.34	12.46 ± 9.23	9.77 ± 5.61	11.99 ± 8.90	13.25 ± 7.07
Coke plant dust	6.93 ± 4.11	16.98 ± 11.7*	6.68 ± 5.06	6.48 ± 3.85	9.39 ± 5.65
Steel plant dust	7.70 ± 4.74	6.99 ± 2.08	6.47 ± 1.82	6.11 ± 2.17	14.29 ± 6.66*

\*: vs. 0 µg/ml,  $P < 0.05$ .

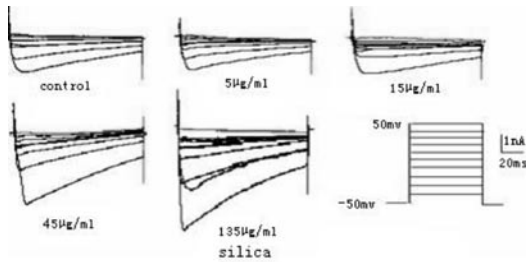


**Figure 1.** Effect of different dose quartz on DRG HVA calcium currents.

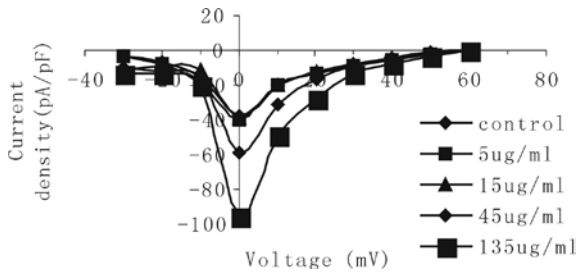


**Figure 2.** The Effects of quartz dust on the DRG HVA calcium currents I-V curve.

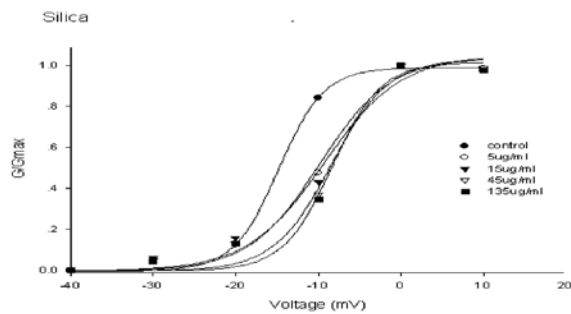


**Figure 3.** Effects of stable state activation curve by different concentrations of quartz on DRG HVA calcium currents.

calcium channel is easy to be activated. In addition, after exposure to particles the tissues produce lipid peroxidation response and free radical; the latter possess negative charge, influences potential sensitivity of S4, and depress

the threshold of activation of HVA calcium channel. S4 is the area for potential sensitivity and directly regulates calcium channel activity by positive charge of spiral arrangement outside of alpha spiral<sup>[7]</sup>. The positive charge may be neutralized or attracted by the negative charge out of silica particle<sup>[8]</sup>, which makes spiral rotate and sensitivity of S4 to potential increase, and the calcium channel is easy to be activated. In addition, after exposure to particles the tissues produce lipid peroxidation response and free radical; the latter possess negative charge, influences potential sensitivity of S4, and depress the threshold of activation of HVA calcium channel.

The effect of various dust was different on DRG HVA calcium channel. The maximum current significantly increased and attenuated quickly. The peak current is mainly related to N type calcium channel, while the last fraction is related to L type calcium channel. This result indicated that N and L type calcium channel might be influenced by silica and it showed a characteristic of activation fast and deactivation fast, which is different from normal L calcium current<sup>[9]</sup>. Dust from coke oven plant and steel plant mainly influenced the activation process of DRG HVA. The difference might be related to the different dust composition<sup>[10]</sup>.

Many researches show that particles are complex. Some elements may activate calcium channels, for instance, ultrafine carbon black and manganese ion can significantly increase the inflow<sup>[11,12]</sup>. While some elements may restrain HVA calcium channels open. Hinkle *et al* reported that half of inflow, produced by depolarization and calcium agonist BAYK8644, was restrained by 4 µmol/L cadmium ion<sup>[13]</sup>. Calcium ion inflow was completely blocked by 1 µmol/L lead ion<sup>[14]</sup>. It was obvious that joint action of several factors should be noticed when we explored the biological effect of particulate matter.

There is a close relation between inflammatory reaction and the change of calcium channel after exposed to dust. Veronesi B *et al* considered that irritant receptors, found on the cell bodies and DRG nerve terminals, are sensitive to a wide range of noxious stimulus (for example, dust). When it is activated, ecto-calcium inflow, cytokines such as neuropeptide and interleukin release, and neuro-

genic inflammation initiate, thus, inflammatory response starts<sup>[15]</sup>.

## 5 Conclusion

Our research showed that silica mediated inflammatory response probably by influencing calcium channel of DRG HVA. It was noticed that inflammation was common course of occupational dust damage (for example, pulmonary fibrosis and tumor). Therefore, a new approach is provided to study damage mechanism of dust by exploring the change of calcium channel in patch clamp technique.

## References

1. Lammers JW, Barnes PJ, Chung KF. Nonadrenergic, noncholinergic airway inhibitory nerves. *Eur Respir J* 1992; 5(2): 239 – 46.
2. Meggs WJ. Neurogenic inflammation and sensitivity to environmental chemicals. *Environ Health Perspect* 1993; 101(3): 234 – 8.
3. Veronesi B, Oortgiesen M, Roy J, *et al.* Particulate matter inflammation and receptor sensitivity are target cell specific. *Inhal Toxicol* 2002; 14(2): 159 – 83.
4. Baluk P. Neurogenic inflammation in skin and airways. *J Investig Dermatol Symp Proc* 1997; 2(1): 76 – 81.
5. Albrecht C, Schins PF, Hohn D, *et al.* Inflammatory time course after quartz instillation: role of tumor necrosis factor- and particle surface. *American Journal of Respiratory Cell and Molecular Biology* 2004; 31: 292 – 301.
6. Yu YQ, Chen J. Voltage gating potassium, calcium, sodium ion channel structure and classification. *China Neurology Medical Journals* 2005; 4 (5): 515 – 20.
7. Chen YH, Li MH, Zhang Y, *et al.* Structural basis of the alpha1-beta subunit interaction of voltage-gated Ca<sup>2+</sup> channels. *Nature* 2004; 429(6992): 675 – 80.
8. Wen HR. Different shape of SiO<sub>2</sub> nature research. *South Jiangxi Normal College Journal* 1994; 1: 43 – 8.
9. Kim SJ, Song SK, Kim J. Inhibitory Effect of nitric oxide on voltage-dependent calcium currents in rat dorsal root ganglia cells. *Biochemical and Biophysical Research Communications* 2000; 271: 509 – 14.
10. Pempkowiak J, Walkusz-Miotk J, Beldowski J, *et al.* Heavy metals in zooplankton from the Southern Baltic. *Chemosphere* 2006; 62(10): 1697 – 708.
11. Stone V, Tuinman M, Vamvakopoulos JE, *et al.* Increased calcium influx in a monocytic cell line on exposure to ultrafine carbon black. *Eur Respir J* 2000; 15(2): 297 – 303.
12. Tracy JM, Colin WT. Extracellular heavy-metal ions stimulate Ca<sup>2+</sup> mobilization in hepatocytes. *Biochem J* 1999; 339: 555 – 61.
13. Hinkle PM, Kinsella PA, Osterhoudt KA. Cadmium uptake and toxicity via voltage-sensitive calcium channels. *J Biol Chem* 1987; 262: 16333 – 7.
14. Garza A, Vega R, Soto E. Cellular mechanisms of lead neurotoxicity. *Med Sci Monit* 2006; 12(3): RA57 – 65.
15. Veronesi B, Oortgiesen M. Neurogenic inflammation and particulate matter (PM) air pollutants. *Neuro Toxicology* 2001; 22: 795 – 810.